Materials Research Express

PAPER

Spontaneous growth of III-nitride 1D and 0D nanostructures on to vertical nanorod arrays

To cite this article: Chirantan Singha *et al* 2019 *Mater. Res. Express* **6** 1050b2

Materials Research Express

PAPER

Spontaneous growth of III-nitride 1D and 0D nanostructures on to vertical nanorod arrays

RECEIVED
11 June 2019

REVISED
7 August 2019

ACCEPTED FOR PUBLICATION
30 August 2019

PUBLISHED
11 September 2019

Chirantan Singha[1], **Sayantani Sen**[1], **Alakananda Das**[2], **Anirban Saha**[2], **Subhrajit Sikdar**[3], **Pallabi Pramanik**[4] **and Anirban Bhattacharyya**[2]

[1] Centre for Research in Nanoscience and Nanotechnology, University of Calcutta, JD2 Sector III Salt Lake City, Kolkata-700106, West Bengal, India
[2] Institute of Radio Physics and Electronics, University of Calcutta, 92 A. P. C. Road, Kolkata-700009, West Bengal, India
[3] Department of Electronic Science, University of Calcutta, 92 A. P. C. Road, Kolkata-700009, West Bengal, India
[4] Department of Electronics and Telecommunication Engineering, Indian Institute of Engineering Science and Technology, Shibpur, Howrah - 711 103, West Bengal, India

E-mail: anirban.rpe@caluniv.ac.in

Keywords: nanostructures, molecular beam epitaxy, nitrides

Abstract

In this work, we report on the growth of AlGaN nanostructures by the droplet epitaxy process. Initially, well-oriented vertical AlN nanorod clusters were grown on to c-plane sapphire substrates by Plasma Assisted Molecular Beam Epitaxy (PA-MBE). On top of these AlN nanorods an $Al_{0.76}Ga_{0.24}N$ layer was deposited, followed by 40 pairs of $Al_{0.76}Ga_{0.24}N$/AlN Multiple Quantum Wells (MQWs). Spontaneously formed nanodots and nanowires were observed by Field Emission Scanning Electron Microscopy (FESEM) on the top planes of these vertical nanorod arrays. For nearly stoichiometric conditions, 20 nm diameter AlGaN nanodots were formed selectively at the step edges generated during step-flow growth. For growth under excess group III conditions, lateral nanowires were formed perpendicular to the edges of the vertical nanorods, with widths varying from 20 nm near the center to 70 nm at the edge for a length of ~150 nm. An enhancement of at least 15 times was obtained in the Cathodoluminescence (CL) emission peak intensity (290 nm) from the top of the nanorod structures. We believe these spontaneously formed well-ordered nanodot and horizontal nanowire structures are generated by the sequential formation and Nitridation of metal nanodroplets on the growth surface. Their properties can be controlled by optimization of the deposition parameters by varying the surface diffusivity of Ga and Al adatoms.

Deep Ultraviolet (DUV) emitters based on III-Nitride materials have been under focus for more than a decade [1, 2]. While commercialization has already occurred, the efficiency of these devices still lags significantly behind the blue emitters [3]. Light Emitting Diodes (LEDs) grown on to single crystal substrates [4], templates [5], or Epitaxial Lateral Overgrowth (ELO) structures [6], show improved efficiency, but the cost increases very significantly. Growth on to comparatively less expensive sapphire substrates lead to large dislocation densities, and point defects associated with them which act as charge traps and non-radiative recombination centers reducing the efficiency. In InGaN based blue LEDs, these defects are mitigated by the spatial localization of carriers [7, 8]. In AlGaN based UV LEDS, this can be replicated through the use of nanodots, where the carriers are confined thereby increasing radiative recombination rates. Such nanodots have been reported using modified Sranski-Krastanov techniques in AlGaN alloys [9, 10]. Another technique for the generation of such structures is droplet epitaxy, which has been reported previously in GaN and InGaN materials [11–13].

A number of recent works [14, 15] have targeted the use of vertical nanostructures of III-Nitride materials for the fabrication of photonic devices, as the defects for such structures are expected to be mostly confined to the surface, which can be passivated. Rigorous preparation steps prior to the growth have led to improved uniformity of diameter and pitch for such nanostructures deposited on novel substrates [16, 17]. Although these methods predict a promising future, the large numbers of steps may hinder large scale fabrication. This can be

avoided if uniform and well oriented vertical nanostructures can be formed spontaneously within the epitaxial layers of III-Nitride materials using traditional growth on to sapphire substrates.

The growth of well oriented AlN vertical nanorods by MBE technique has been already reported [18, 19]. Controlled modification of surface diffusion lengths of adatoms can lead to the spontaneous growth of such nanostructures within epitaxial layers. In this work, we report on the growth of $Al_{0.76}Ga_{0.24}N/AlN$ Multiple Quantum Wells (MQWs) on top of such vertical nanorods. The optical properties of such layers were compared to similar structures grown on continuous films.

All samples considered here were grown by Plasma-Assisted Molecular Beam Epitaxy (PA-MBE) method using a VEECO Gen-930 system. The substrate used for the growth was c-plane single side polished sapphire (Monocrystal, Russia) of 2 inch diameter and 300 μm thickness. The substrates were outgassed at 140 °C at the entry chamber and then at a temperature of 400 °C at 10^{-9}T pressure prior to the growth. The substrate temperature was maintained at 800 °C during the growth.

The three-step growth process was initiated with nitridation of the sapphire substrate. The Nitrogen was activated using an RF plasma source (UNI-Bulb) which was operated at a power of 400 W. A flow rate of 1.7 sccm of high purity nitrogen gas was employed for all layers, even though the plasma power was varied. Subsequently, an AlN buffer layer of 100 nm thickness was grown to mitigate the lattice mismatch. An $Al_{0.76}Ga_{0.24}N$ thin film of about 1 μm thickness was grown on top of this buffer layer. Finally, 40 pairs of $Al_{0.76}Ga_{0.24}N/AlN$ Multiple Quantum Well (MQW) structures were grown with wells nominally 8 Mono Layers (ML) wide and barriers 11 MLs wide. For all these layers grown after the nitridation of the substrate, the RF plasma power employed was 350 W and the other parameters related to the active nitrogen plasma were unchanged. The growth rate is typically 0.25 μm per hour under these conditions. In this paper, we study two samples M1 and M2, which were grown using different group III to group V flux ratio, as described in the following section.

The growth was characterized *in situ* using Reflection High Energy Electron Diffraction (RHEED) system during the process. The surface morphology of the grown sample was studied using a Zeiss Auriga Field Emission Scanning Electron Microscope (FESEM) system. GATAN MONOCL4 system mounted on to a JSM 7600 F Scanning Electron Microscope (SEM) was used for the cathodoluminescence (CL) measurements. 9 KW Rigaku SmartLab x-ray Diffractometer was used for the High Resolution x-ray Diffraction (HRXRD) studies.

Growth of AlGaN is typically carried out under excess group III, that is, under metal-rich conditions. However, since the arrival rate of active nitrogen depends in a complex fashion on the pressure inside the RF source, flow rates, and applied RF bias, it is difficult to directly quantify the group III to group V flux ratio. We have estimated this very important growth parameter indirectly through the growth of AlGaN alloys under excess group III conditions, and measuring their alloy composition by subsequent XRD studies. During the growth of AlGaN alloys by PAMBE, the sticking coefficient of Al is nearly unity at the substrate temperature employed in this work, 800 °C, while that for Ga is significantly lower. This, along with the stronger Al-N bond ensures that the AlN mole fraction is determined by the ratio of the Al flux employed, as measured by the Beam Equivalent pressure (BEP) to that required for stoichiometric growth of AlN. Therefore, by carrying out a series of growths of AlGaN thin films under the same group V conditions, and measuring their AlN mole fractions, the Al BEP necessary for stoichiometric growth was determined, thereby enabling us to quantify group III to group V flux ratio, subsequently. Based on these calibrations, we estimate the BEP corresponding to stoichiometric growth of AlN to be 1×10^{-7} T.

Initial work involved the growth of vertical AlN nanorods on sapphire, by optimization of the buffer layer deposition conditions. Deposition was carried out in a mode involving a periodic deposition-nitridation scheme, and variations were made in the Al flux employed for the AlN buffer layers. The buffer layers were grown under constant active nitrogen, while the Al flux was switched on and off. The BEP of Al was chosen to be higher than that necessary for stoichiometric growth, and Al shutter was opened initially for a period (T_{on}) of ~20 s (6 ML), after which it was closed for a similar time period (T_{off}) when the deposited Al was exposed to the plasma. The RHEED pattern was dim and diffused when the Al shutter was open, and during the subsequent exposure step it became clear, that is the contrast increased, indicating that the excess Al metal on the surface has been converted to AlN. The time period chosen for the T_{off} was such that the RHEED evolution was complete indicating that full conversion of the metallic layer to semiconductor was completed. This process was repeated with progressively longer T_{on} values, which required longer T_{off} values for complete conversion. Specifically for sample M1 the AlN buffer layer was grown using an Al cell temperature of 1110 °C, with a corresponding BEP of 2.19×10^{-7} T (219% of stoichiometric value). Sample M2, was also grown under excess group III but the group III to group V flux ratio was significantly lower than M1. The AlN buffer layer was deposited using an Al temperature of 1080 °C corresponding to a BEP of 1.18×10^{-7} T, which is slightly Al rich, 118% of the stoichiometric value. For this sample shorter T_{off} times were required for the same T_{on} times for complete conversion. A total time of ~5 min was employed during this nucleation step for both the samples. Subsequent to the nucleation step, AlN layer was deposited in a conventional manner, without any interruption for 20 min and 10 min respectively for the two samples M1 and M2.

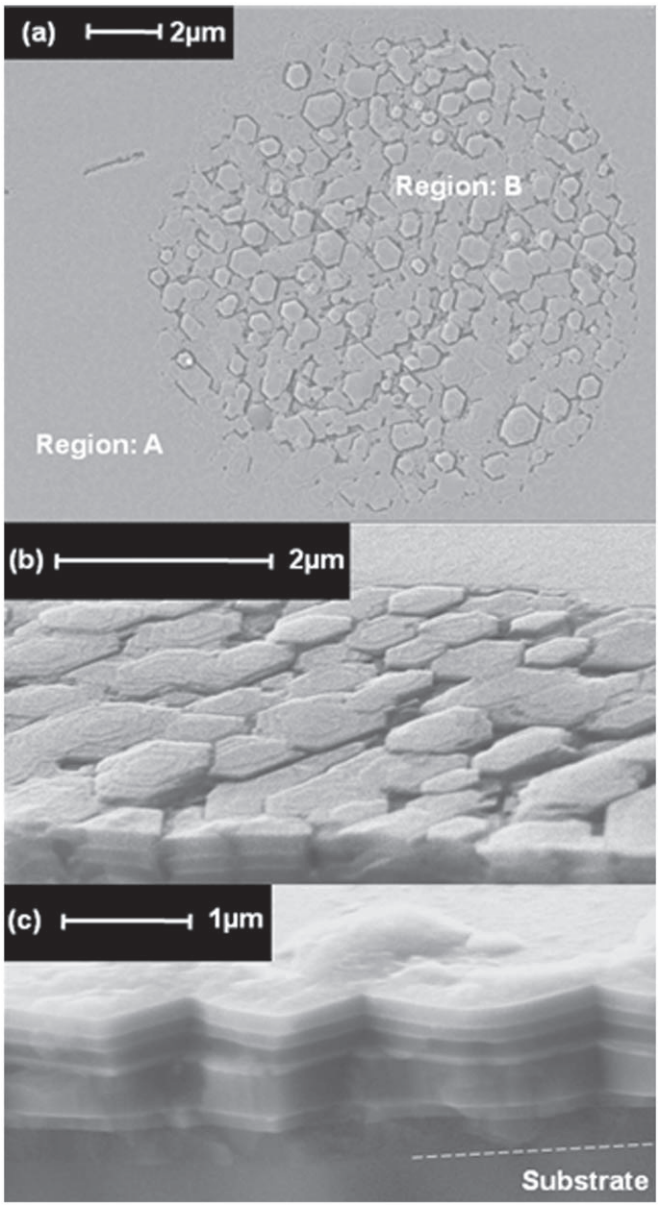

Figure 1. FESEM image of (a) the surface and (b) and (c) the cross section of the sample M1.

Subsequently, an AlGaN layer was deposited with Al cell temperature of 1060 °C, corresponding to an Al BEP of 7.53×10^{-8} T. During the growth of the bulk AlGaN layer for the sample M1, the gallium BEP was ramped from 6.84×10^{-7} T (1080 °C) to 9.73×10^{-7} T (1100 °C). For sample M2, the gallium cell temperature employed was 1060 °C corresponding to a BEP of 4.5×10^{-7} T. While growing these structures, since the excess gallium stays on the surface, a number of growth interruption steps were introduced, where the metal shutters were closed and the surface was exposed to the active nitrogen for a period of time. During this period, the metallic layer is either desorbed or incorporated into the film. The composition of these deliberately introduced interlayers is expected to be of higher gallium content than the overall AlGaN film.

Finally, a set of 40 MQWs were deposited, with $Al_{0.76}Ga_{0.24}N$ wells and AlN barriers. The conditions for deposition of the well materials for sample M1 and M2 are similar to that employed in the underlying AlGaN layer, that is the Ga flux was significantly higher in M1 than in M2. It should be noted here that subsequent to the completion of each stages the surface was exposed to the active nitrogen, so that any excess group III materials present on the surface would be consumed and converted to III-Nitride films.

Post growth examination of the surface morphology by FESEM (figure 1(a)) for sample M1 indicates that while the surface is generally smooth (Region A), there are a large number of small circular features present (Region B) containing clusters of vertically oriented nanorods of clear hexagonal cross-sections and diameters ranging from 300 nm to 1 micron. Cross-sectional FESEM image for these nanorods structures at two different magnifications is shown in figures 1(b) and (c). The interface of the sapphire and AlN layer is highlighted using a

dotted line for easy identification. In figure 1(b) we can observe a portion of the surface where the nanorods clusters designated as Region B are clearly observed. At higher magnification, the clearly observed facet side-walls (figure 1(c)) further confirm that the vertical nanorods originate from the initial nucleation region and grow without any change in the diameter. While at this magnification the quantum wells cannot be identified, several layers can be observed. These originate when growth interruptions were carried out during the deposition of the thick AlGaN layer, as will be discussed later.

The variation of the group III flux for the two samples M1 and M2 leads to a clearly observed difference in the nanorods structures. For sample M1, the cluster size and nanorods diameters range from 5 μm to 15 μm and 300 nm to 1 μm respectively. For M2, which used significantly lower Al flux in the nucleation stage, the corresponding numbers are 3 μm to 4 μm and 200 nm to 400 nm. Moreover, the density of these clusters are significantly lower for sample M1 (300 mm^{-2}) than M2 (1E4 mm^{-2}). Thus we can conclude that higher Al flux leads to larger clusters, but with lower densities. Furthermore, the nanorods diameter also increased with increasing Al flux.

From these results we conclude that the nucleation of these nanorod clusters originate from the initial AlN nucleation step, and is directly correlated to the Al flux employed. Both of these samples were grown under excess Al conditions, and due to the low evaporation probability the metal stays on the growth surface. Beyond a thickness, the metallic layer forms nanoscale Al droplets driven by the minimization of surface energy. As mentioned previously, during the buffer layer deposition, the metal shutter was intermittently switched on and off. While the thickness of the metallic layer, and hence the diameter of the Al nanoscale droplets can be controlled by both the arriving flux rate and the time of deposition T_{on}, the second parameter was not changed between M1 and M2. However even for the same T_{on}, the T_{off} was higher for sample M1 as mentioned previously. During the plasma exposure step, the Al metallic droplets were 'frozen' by conversion to AlN, and subsequently formed the nanorods clusters during further deposition. The variation of the cluster size and density therefore varies with the Al BEP employed due to the processes of Al adatom surface diffusion, coalescence and small but finite evaporation rate. The higher Al flux led to a thicker Al film, hence the probability of coalescence increased, leading to a larger cluster diameter but smaller number density.

The HRXRD data for the sample M1 and M2 is shown in figure 2(a). The data for sample M1 is multiplied by 10 to separate the two for better observation. We note that even though a higher Ga flux was employed during the AlGaN layer in sample M1, this does not affect the overall alloy composition, and the peak corresponding to the AlGaN layer indicates that the AlN mole fraction for both the samples is 76%. This is a direct result of the postulate that the composition of AlGaN films grown by PAMBE under excess group III conditions is given by the ratio of the Al flux employed and the Al flux necessary for the growth of stoichiometric AlN, and is independent of the Ga flux [20, 21]. Furthermore, this allows us to calculate the group III to V flux ratios as indicated earlier.

In the XRD plot, along with the peak for AlN buffer layer, clear superlattice peaks are observed for both samples, which correspond to the presence of wells and barriers. It should be noted that for both samples, the periodicity is about 4.4 nm as established from the superlattice peak positions. The superlattice peaks are stronger for sample M1, which was grown using higher gallium flux. This can be linked to the higher degree of interface flatness expected for such growth mode. For sample M1 there is an additional broad peak which corresponds to GaN, but with tails extending to higher values of 2θ. During the deposition of the thick AlGaN layer for both the samples, several growth interruptions were carried out, when the group III shutters were closed and the surface was exposed to the active nitrogen. The metallic layer present on the growth surface partially desorbs and the rest is converted to semiconductor thin films, which can be observed in the cross sectional FESEM (figure 1(c)). From the XRD data we can see that these interruptions produced thin layers of GaN and AlGaN alloys with very low Al content. This peak is absent for sample M2, grown under a significantly lower Ga flux, and thus for M2 the metallic build-up on the growth surface was much less.

On the basis of the above experimental information from both the FESEM and the XRD a schematic of the samples was developed (figure 2(b)). The AlN nanorods shown here were formed during the growth of the AlN buffer. The AlGaN with various interlayers was deposited subsequently, followed by the MQW structures. The FESEM images also indicate that there is a small growth rate difference between two regions, thin film and nanorods bundles, which may give rise to a small variation in MQW periodicities. Furthermore, the crystalline quality and the presence of point defect states are also expected to be different for MQWs grown on these two regions. Finally, from low resolution FESEM images, it is clear that the top of the nanorods is flat with the presence of clear step-like features. This morphology is expected to strongly control the surface mobility of arriving species. This was studied in further detail by high resolution FESEM and the results are presented subsequently.

AlGaN/AlN MQWs deposited on to the vertical nanorods structures were studied by High magnification FESEM. Images obtained from the top hexagonal basal-plane surfaces of the vertical nanorods of sample M2 are presented in figure 3(a). Presence of surface steps can be clearly observed, and the step size for these samples is

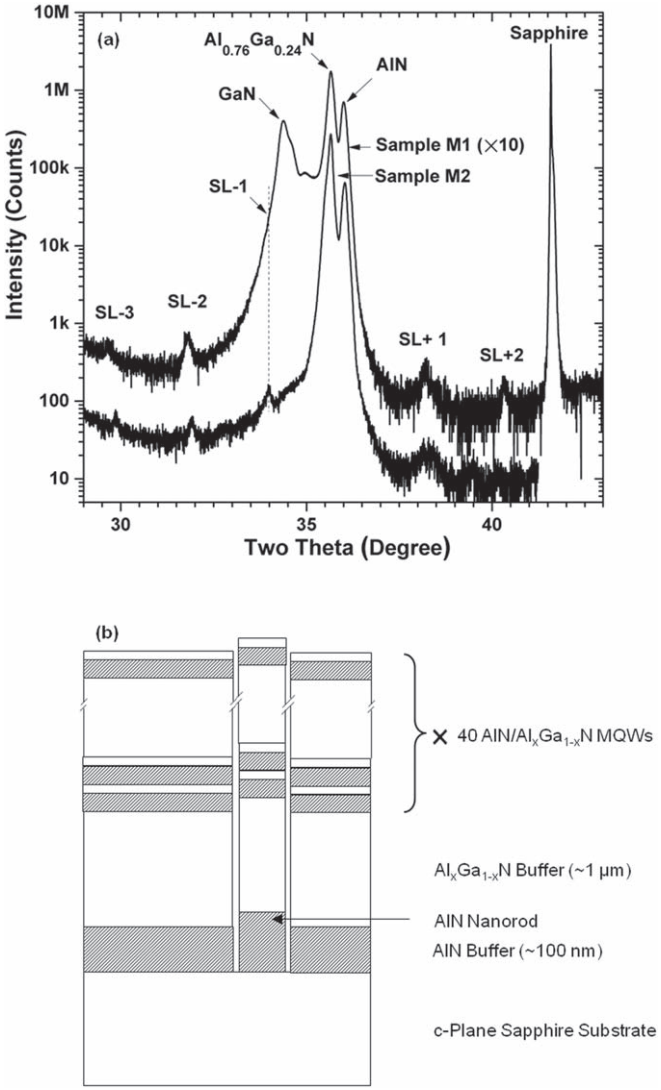

Figure 2. (a) HRXRD data of sample M1 and M2 (b) Schematic diagram of the samples.

about 25 nm. The surface was found to be decorated with the presence of nanodot structures formed selectively at the edges formed by the step flow growth. These structures are about 20 nm in diameter, and show a very narrow size distribution.

We believe that these nanodots are formed by the process of droplet epitaxy. The growth of the AlGaN wells on top of the nanorod structures was carried out under excess group III conditions. The Al flux employed during the deposition of AlGaN layer was ~76% of Al flux required for growth of stoichiometric AlN. However, the gallium flux employed was higher than that required for consumption of the active nitrogen leftover after reaction with Al. Even though a large fraction of the excess gallium evaporates at the growth temperature, the rest forms a metallic layer of the growth surface. The Al flux arriving on the surface is incorporated into the film, forming a metallic alloy [22]. The active nitrogen reacts with the metallic layer forming the III-Nitride film, which subsequently deposits on to the underlying layer epitaxially.

The formation of the nanodots can be linked to metallic alloy film on the growth surface. Due to surface energy minimization, this film spontaneously forms nanoscale droplets, which has been previously reported for GaN on sapphire [11]. In the current situation, the AlGaN droplets, upon reaction with the active nitrogen, forms nanodots as observed in figure 3(a). The diameter and density of such features are controlled by the surface diffusion of the adatoms, coalescence processes as well as desorption, which in turn depends on surface to volume ratio of the droplets. Such ordered lines of quantum dots as observed here are expected to have extensive applications in electronic and memory devices.

The FESEM image of the surface of sample M1 is presented in figure 3(b). We recall that in sample M1, the group III to group V ratio is significantly higher than in sample M2. In this case, we find that that the geometry of these nanostructures formed on top of the vertical nanorods follow the features of the underlying surface, which

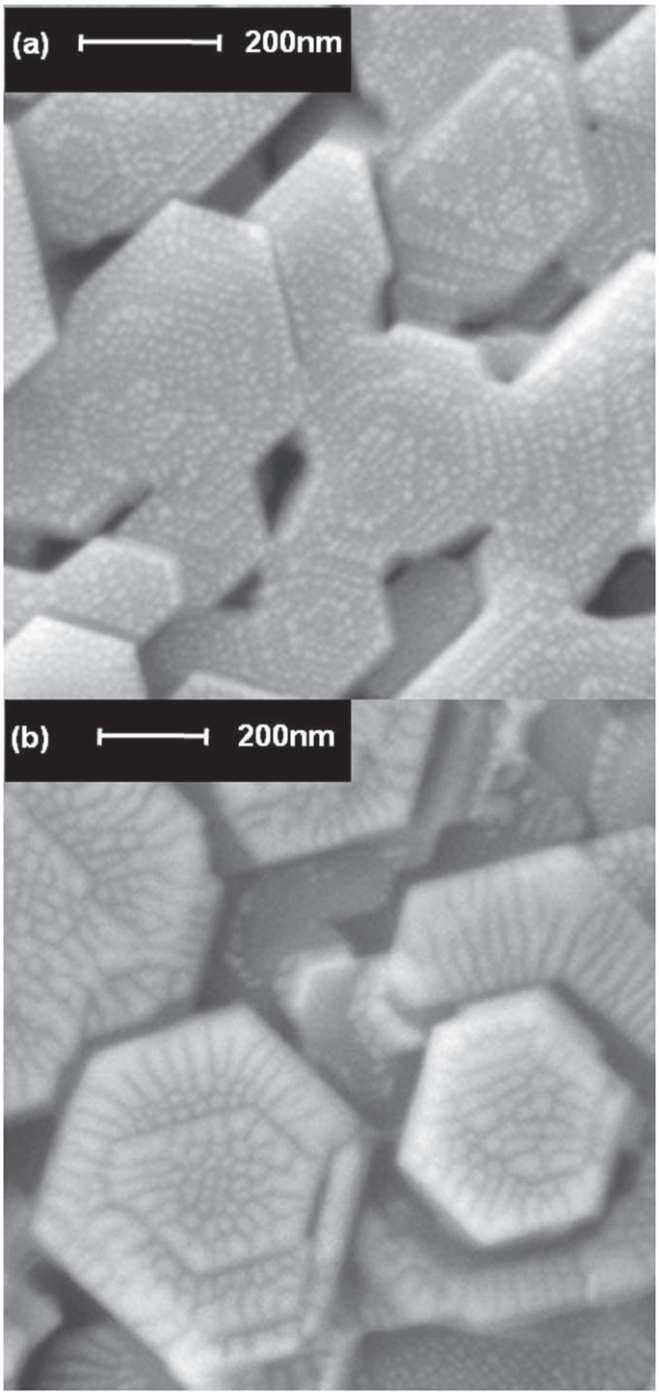

Figure 3. FESEM image of the (a) 0D nanostructures (nanodots) and (b) 1D nanostructures (nanowires).

is the hexagonal basal plane. Near the step edges, the features are horizontal nanowires with their major axis perpendicular to the edge. They are however not cylindrical, but expand out from the center of the nanorod to the edge. The lengths of these structures are typically ~150 nm and the width ranges from 50 nm to 70 nm at the edge. Far away from the edges, however the features are more symmetric and are similar to features observed on sample M2.

We believe that these structures are AlGaN nanodots and nanowires, which were formed during the growth of III-Nitride layers under excess group III and subsequent exposure to active nitrogen. In this case, unlike the nucleation layers which generated the AlN nanorods, the Al flux is much lower than that necessary to consume the active nitrogen. However the gallium flux is significantly higher than necessary and similar effects are observed. In this case, however the depositions are significantly shorter and the gallium desorption is quite high at the growth temperature, which precludes the possibility of a large metallic layer build-up. Consequently, the nanoscale features formed during this growth is significantly smaller. The composition of these nanostructures

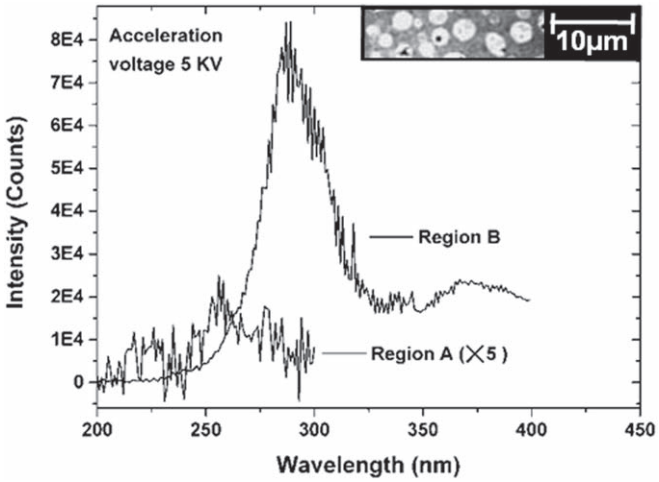

Figure 4. CL spectra of the sample with acceleration voltage 5 KV. Inset: CL image of the sample surface.

is difficult to attribute directly. Experimental evidence based on EDX measurements on such structures grown on a significantly larger scale has shown a lateral variation of alloy composition [18], which was attributed to the competing processes of evaporation and nitridation.

The arrival of the metallic gallium or aluminium at the center of the feature leads to the formation of nanoscale liquid droplets, which subsequently travels towards the edge of the nanorods due to thermal and surface energies. The driving force for the formation of these features is the minimization of surface energy by accumulation of metal layer at the edge of geometrical features, either step edges, or the edge of the nanorod itself. This causes diffusion from the center of the nanorods surface towards the edge, causing an interplay of these processes of desorption and reaction of metal with active nitrogen during the transport. Features far from the edge are symmetric, as the driving force is weaker, and they form nanoscale droplets which react with active nitrogen to form nanodots. At the edge itself, the metal piles up and re-form as the nanoscale metallic droplet, and that also is converted to nanodots. In the region in between, reaction occurs during the transport stage and nanowire like features are developed, whose width reflects the increasing size of the droplet as it moves across the top surface of the nanorod, all the while reacting with active nitrogen to form AlGaN. From these results, a quantitative model of surface diffusion can be developed, which is a subject of a subsequent publication.

Emission properties from two different regions of the samples were determined by cathodoluminescence measurements using an acceleration voltage of 5 KV as shown in figure 4. One of the two regions chosen consisted of the vertical nanorod structures and the other without such structures as indicated in figure 1(a) by 'Region B' and 'Region A' respectively. Oto *et al* [23] has calculated the penetration of the CL into high Al-content AlGaN structures similar to those considered for the current work. They report that while for an acceleration voltage of 8 KV the electrons interact up to a depth of 700 nm, 50% of the energy is lost within the first 100 nm. For 5 KV, the excitation is expected to be limited significantly within the MQW structure which is about 200 nm thick. We observe that the CL peak obtained from top of the nanorod clusters (Region B) is at 289 nm, and is at least 15 times brighter than that measured outside the nanorod region (Region A). Furthermore this peak is red-shifted by about 30 nm, which along with the increase in intensity, is similar to AlGaN MQWs reported in the literature where compositional inhomogeneity was present [24, 25]. The optical transitions for such structures occur from localized minima in the conduction and valence bands where the carriers are localized away from defect states. The exact mechanism for generation of such compositional inhomogeneity is difficult to attribute, may be linked to the step flow growth mode observed on the top of the nanorods and variation of surface diffusion lengths associated with it.

This improvement of the brightness from the top surface of the nanorod structures is also evident from the CL image of the sample surface as presented in the inset of figure 4. The increment of the brightness can be linked to the lower defect density on top of nanorods, which enhances the internal quantum efficiency. Alternatively, this can be also related to the enhancement of extraction efficiency arising from guided optical modes. Further studies are needed to separate out the two effects, and are beyond the scope of the current publication.

A relatively weak extension of the luminescence tail beyond the band-gap of GaN has been observed for the spectra presented in figure 4. We can rule out their origin from defect states, as the ratio of the main peak to this tail remains relatively unchanged with temperature as will be published elsewhere. However, the fact that this peak extends beyond the bandgap of GaN indicates that it originates from GaN structures which are under

significant strain, which causes a red-shift due to quantum confined Stark effect. Thus, a small portion of the nanostructures formed may be nearly GaN.

Conclusions

In this paper we report on a novel technique based on droplet epitaxy for the spontaneous formation of AlGaN nanodots and nanowires by PA-MBE. These were deposited on top of well oriented vertical AlN nanorod structures. For nearly stoichiometric conditions, their top surface was decorated by nanodots formed exclusively at the edges of steps formed during the epitaxial growth. Under excess group III, the dots are elongated along directions perpendicular to the edge of the vertical nanorods, and formed tapered radial nanowires. We attribute the formation of these structures to droplet epitaxy, where nanoscale Al + Ga metallic droplets are nitridated by the active nitrogen plasma. Their dimension and nature depends on the surface diffusion of adatoms, coalescence of droplets and reaction rates. The CL intensity obtained from these vertical nanorods is significantly brighter, and these results are likely to be very useful for optoelectronic devices that employ quantum dots as the active region.

Acknowledgments

This work was partially funded by the Department of Information Technology (12(3)/2011-PDD), Government of India and by the Office of the Principal Scientific Advisor to the Government of India (Prn SA/W-UV LEDs/2017). Chirantan Singha would like to acknowledge the Department of Science and Technology (DST) INSPIRE fellowship (IF120257), Sayantani Sen (09/028(0921)/2014-EMR-I), and Alakananda Das (09/028 (0946)/2015-EMR-I) would like to acknowledge the Council of Scientific and Industrial Research (CSIR) Senior Research Fellowship scheme. Pallabi Pramanik would like to acknowledge SERB-National Postdoctoral Fellowship (SERB-NPDF, Government of India: PDF/2017/001605). Anirban Saha and Subhrajit Sikdar would like to acknowledge UGC for funding their work.

ORCID iDs

Anirban Bhattacharyya https://orcid.org/0000-0002-8276-0403

References

[1] Moustakas T D and Paiella R 2017 *Rep. Prog. Phys.* **80** 106501
[2] Hirayama H 2005 *J. Appl. Phys.* **97** 091101
[3] Kneissl M *et al* 2011 *Semicond. Sci. Technol.* **26** 014036
[4] Grandusky J R, Chen J, Gibb S R, Mendrick M C, Moe C G, Rodak L, Garrett G A, Wraback M and Schowalter L J 2013 *Appl. Phys. Express* **6** 032101
[5] Sumiya S, Zhu Y, Zhang J, Kosaka K, Miyoshi M, Shibata T, Tanaka M and Egawa T 2008 *Jpn. J. Appl. Phys.* **47** 43
[6] Kamiyama S, Iwaya M, Takanami S, Terao S, Miyazaki A, Amano H and Akasaki I 2002 *Phys. Stat. Sol.* (a) **192** 296–300
[7] Chichibu S, Azuhata T, Sota T and Nakamura S 1996 *Appl. Phys. Lett.* **69** 4188–90
[8] Nakamura S 1998 *Science* **281** 956–61
[9] Brault J *et al* 2018 *Semicond. Sci. Technol.* **33** 075007
[10] Himwas C, den Hertog M, Bellet-Amalric E, Songmuang R, Donatini F, Dang L S and Monroy E 2014 *J. Appl. Phys.* **116** 023502
[11] Özcan A S, Wang Y, Ozaydin G, Ludwig K F, Bhattacharyya A, Moustakas T D and Siddons D P 2006 *J. Appl. Phys.* **100** 084307
[12] Kawasaki K, Yamazaki D, Kinoshita A, Hirayama H, Tsutsui K and Aoyagi Y 2001 *Appl. Phys. Lett.* **79** 2243
[13] Oliver R A, El-Ella H A R, Collins D P, Reid B, Zhang Y, Christie F, Kappers M J and Taylor R A 2013 *Materials Science and Engineering* B **178** 1390–4
[14] Zhao S *et al* 2015 *Sci. Rep.* **5** 8332
[15] Le B H, Liu X, Tran N H, Zhao S and Mi Z 2019 *Opt. Express* **27** 5843
[16] Zhao S and Mi Z 2018 *IEEE J. Quantum Electron.* **54** 2001009
[17] Sun H and Li X 2019 *Phys. Status Solidi* A **216** 1800420
[18] Singha C, Sen S, Pramanik P, Palit M, Das A, Roy A S, Sen S and Bhattacharyya A 2018 *J. Cryst. Growth* **481** 40–7
[19] Landré O, Fellmann V, Jaffrennou P, Bougerol C, Renevier H, Cros A and Daudin B 2010 *Appl. Phys. Lett.* **96** 061912
[20] Wang Y, Özcan A S, Ludwig K F, Bhattacharyya A, Moustakas T D, Zhou L and Smith D J 2006 *Appl. Phys. Lett.* **88** 181915
[21] Iliopoulos E and Moustakas T D 2002 *Appl. Phys. Lett.* **81** 295
[22] Moustakas T D and Bhattacharyya A 2011 *ECS Trans.* **35** 63–71
[23] Oto T, Banal R G, Kataoka K, Funato M and Kawakami Y 2010 *Nat. Photonics* **4** 767–70
[24] Pramanik P, Sen S, Singha C, Roy A S, Das A, Sen S, Bhattacharyya A, Kumar D and Rao D V S 2016 *J. Cryst. Growth* **439** 60
[25] Sampath A V, Garrett G A, Enck R W, Rotella P Jr, Shen H and Wraback M 2011 *Phys. Status Solidi* C **8** 1534–8